ELSEVIER

www.elsevier.com/locate/ica
Inorganica Chimica Acta 329 (2002) 129–134

Inorganica Chimica Acta

Note

Iron–iron interaction through an ethanedithiolate ligand: a magnetic and theoretical study

Karine Costuas [a], Maria Luisa Valenzuela [b], Andres Vega [c], Yanko Moreno [c], Octavio Peña [a], Evgenia Spodine [c,*], Jean-Yves Saillard [a,*], Carlos Diaz [b,*]

[a] *Laboratoire de Chimie du Solide et Inorganique Moléculaire, UMR-CNRS 6511, Institut de Chimie de Rennes, Université de Rennes 1, 35042 Rennes Cedex, France*

[b] *Departamento de Quimica, Facultad de Ciencias, Universidad de Chile, Casilla 653, Santiago, Chile*

[c] *Facultad de Ciencias Quimicas y Farmaceuticas and Centro para la Investigation Interdisciplinaria Avanzada en Ciencia de los Materiales Universidad de Chile, Casilla 233, Santiago, Chile*

Received 17 June 2001; accepted 5 October 2001

Abstract

The compound ([CpFe(dppe)]$_2$[μ-SCH$_2$CH$_2$S–S,S′])(PF$_6$)$_2$ ([**1**][PF$_6$]$_2$) has been synthesized and its magnetic properties have been investigated by susceptometer quantum interface device (SQUID) measurements in the temperature range 5–300 K. The d^5–d^5 $\mathbf{1}^{2+}$ complex exhibits intramolecular antiferromagnetic behavior, with a magnetic coupling constant of -6.4 cm^{-1}. Density functional theory (DFT) calculations on a model of $\mathbf{1}^{2+}$ (as well as on models of $\mathbf{1}^{+}$ and **1**) allow to determine its molecular structure and analyse its bonding and magnetic properties. The computed spin density exhibits significant localization on both the Fe and S centers. Replacing the heteroatoms of the bridging ligand by CH$_2$ groups leads to a relocalization of the spin density on the metal atoms and favors ferromagnetic coupling.

Keywords: Magnetic properties; Iron complexes; Dithiolate complexes

1. Introduction

Complexes having electronic and magnetic interaction between metal centers through thiolate ligands have attracted the attention because they provide model compounds for biologically redox active metalloproteins [1]. Among the thiolate ligands [2,3], few complexes with ethanedithiolate as bridging units have been reported. The ethane-1,2-dithiolate ligand is known to exhibit diverse coordination modes [4,5]. Surprisingly, although numerous examples of complexes containing chelating ethane-1,2-dithiolate have been reported [4,6], only a small amount of metal compounds containing linear M[μ-S(CH$_2$)$_n$S–S,S′]M bridges have been synthesized. We have previously reported investigations of metal–metal electronic and magnetic interactions through several bridging ligands [7–10]. In this paper, we report the synthesis, magnetic investigation as well as a density functional theory (DFT) study of ([CpFe(dppe)]$_2$[μ-SCH$_2$CH$_2$S–S,S′])(PF$_6$)$_2$ ([**1**][PF$_6$]$_2$). Due to the impossibility for obtaining suitable single crystals of any salt of ([CpFe^{III}(dppe)]$_2$[μ-SCH$_2$-CH$_2$S–S,S′])$^{2+}$ ($\mathbf{1}^{2+}$), it was not possible to determine its X-ray molecular structure. Nevertheless, we were able to determine a molecular structure by carrying DFT geometry optimizations. To the best of our knowledge, this is the first characterized iron dinuclear organometallic compound which contains a μ-dithiolato ligand.

2. Experimental

All reactions were carried out under N$_2$, using standard Schlenk techniques. Solvent were purified using standard procedures. Infrared spectra were recorded on a Perkin–Elmer FT-IR 2000 spectrophotometer. Elemental analysis were performed with a Perkin–Elmer 240 microanalyser. Visible absorption spectra were

* Corresponding authors. Tel.: +33-299-286 123; fax: +33-299-635 704 (J.-Y.S.).

0020-1693/02/$ - see front matter
PII: S0020-1693(01)00734-4

measured on a Varian DMS-90 in 1 cm cuvettes. Magnetic susceptibility measurements were performed with a SHE 906 SQUID (susceptometer quantum interface device) instrument in the temperature range 5–300 K. The applied field was 1 Koe. Pascal's constants were used to estimate the corrections for the underlying diamagnetism of the sample.

2.1. Preparation of $[CpFe(dppe)–S(CH_2)_2S–CpFe(dppe)](PF_6)_2$

The $[\mathbf{1}][PF_6]_2$ salt was prepared according to a previously reported method [11], from the reaction of CpFe(dppe)I with $HS(CH_2)_2SH$ in the presence of NH_4PF_6 using CH_3OH as solvent. FT-IR (KBr, cm^{-1}) 1097 (δ(C–H)$_{ip}$, C_5H_5); 699 (δ(C–H)$_{op}$, C_6H_6dppe); 847 ($\nu(PF_6)$). UV(CH_3OH): λ_{max} (nm) = 429,593.

3. Computational details

DFT calculations [12] were carried out using the Amsterdam Density Functional (ADF) program [13] on the model compounds ($[CpFe(dpe)]_2[\mu\text{-}SCH_2CH_2S–S,S']^{n+}$ ($Cp = \eta^5\text{-}C_5H_5$; $dpe = \eta^2\text{-}H_2PCH_2CH_2PH_2$, $n = 0–2$) ($\mathbf{1}'^{n+}$) and ($[CpFe(dpe)]_2[\mu\text{-}CH_2–CH_2CH_2–CH_2–C,C']^{n+}$ (2^{n+}). The Vosko–Wilk–Nusair parametrization [14] was used to treat electron correlation within the local density approximation (LDA). The following corrections to the LDA functional were applied: The Stoll correction [15] to the correlation energy and non-local corrections to the exchange and correlation energies of Perdew-Wang91 [16] (Stoll-PW91). The numerical integration procedure applied for the calculations was developed by Velde and co-workers [12c]. The basis set used for Fe was a triple-ζ Slater-type orbital (STO) basis for Fe 3d and 4s, and a single-ζ 4p function. Concerning S and C atoms of the thiolate bridge, a triple-ζ STO basis set was employed for C 2s and 2p, S 3s and 3p, extended with a single-ζ polarization function (3d). The other atoms were described by a double-ζ STO basis set for H 1s, C 2s and 2p, and P 3s and 3p, augmented with a single-ζ polarization function (2p for H, C; 3d for P). Geometry optimizations (assuming C_1 symmetry) were carried out on each complex, using the analytical gradient method implemented by Verluis and Ziegler [17]. The optimized geometries giving rise to the more stable conformers showed no significant deviation from C_i symmetry. Spin-unrestricted calculations were performed for all the considered open-shell systems on various possible rotational conformations. Calculations using the broken symmetry (BS) approach [18], which consists in performing spin-unrestricted calculations on low-spin open-shell systems without any symmetry constraint connecting the magnetic centers and imposing an asymmetry in the starting spin density, were carried out on the singlet states of the considered bications. Unlike spin-restricted calculations, the BS approach allows the α and β spin densities of the singlet state to localize on different parts of the molecule.

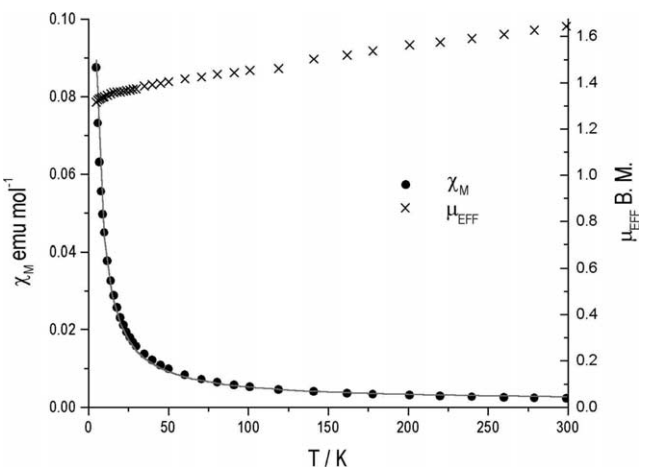

Fig. 1. Temperature dependence of the molar magnetic susceptibility and of the magnetic moment per Fe atom for compound $[\mathbf{1}](PF_6)_2$. Full line corresponds to the fit of magnetic data with the Bleaney–Bowers equation.

4. Results and discussion

Fig. 1 shows the temperature dependence of the magnetic susceptibility of the paramagnetic dinuclear $\mathbf{1}^{2+}$ cation. This 17-electron d^5–d^5 Fe^{III} dinuclear complex presents a magnetic moment per iron metal center of $1.64\mu_B$ at room temperature. This magnetic moment decreases as the temperature is lowered and reaches a value of $1.32\mu_B$ at 5 K. An apparent intramolecular antiferromagnetic behavior of $\mathbf{1}^{2+}$ can be inferred from the lowering of the magnetic moment with the decrease of temperature. In order to postulate an intramolecular exchange interaction the magnetic susceptibility data were fitted with the modified Bleaney–Bowers equation [19] for exchange-coupled pairs of ions with $S = \frac{1}{2}$, based on the spin–Hamiltonian $-2JS_1S_2$

$$\chi_M = \frac{N\beta^2g^2}{3k(T-\theta)}\left\{1+\frac{1}{3}\left\{\exp\left(\frac{-2J}{kT}\right)\right\}\right\}^{-1}(1-\rho) + \frac{N\beta^2g^2}{4kT}\rho + \chi_o$$

In this expression all symbols have their usual meaning, χ_M is expressed per mole of dimer, θ is a Weiss-like correction to account for possible intermolecular exchange effects. These corrections are usually small and may result from weak lattice associations or hydrogen-bonding interactions. The impurities, ρ, are modeled as a Curie paramagnet. χ_o corresponds to the temperature independent paramagnetism (TIP).

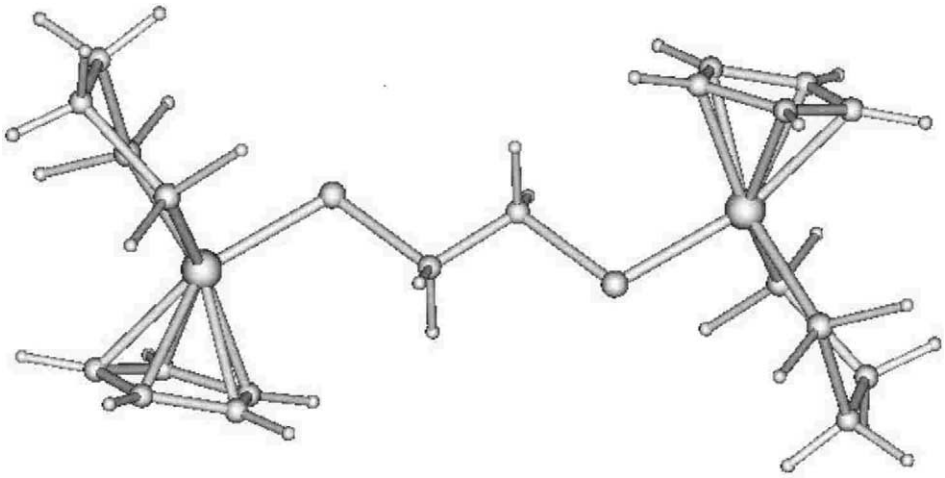

Fig. 2. DFT optimized molecular structure of $\mathbf{1}'^{2+}$ in its C_i singlet state (see computational details).

The parameters giving the best fit were obtained by using a non-linear regression analysis. The values of these parameters are: $g = 2.02$, $\theta = 0$ K, $2J = -6.4$ cm^{-1}, $\rho = 5\%$, $\chi_o = 148 \times 10^{-5}$. The obtained g value is close to the experimental value of 2.07, calculated from the powder EPR spectrum of $[\mathbf{1}][PF_6]_2$ [20]. The low singlet–triplet gap indicates that the studied complex is weakly coupled, with a singlet ground state in close proximity to the triplet state. The observed value of the magnetic moment at room temperature is similar to the one informed for the discrete monomeric 17-electron d^7 iron complex, Cp*Fe(dppe) [21], and does not correspond to the typical behavior of 'Werner' low-spin Fe^{III} complexes with a t_{2g}^5 configuration. The latter usually have orbital contributions to their moments at room temperature, thus presenting values of approximately $2.3\mu_B$ [22]. On the other hand, similar magnetic interactions between Cp*Fe(dppe) centers through conjugated carbon bridges have been reported [21b,21c].

In order to determine the molecular structure of $\mathbf{1}^{2+}$, to analyse its bonding and to explain its magnetic behavior, DFT calculations were undertaken on the simplified models $\mathbf{1}'$, $\mathbf{1}'^{+}$ and $\mathbf{1}'^{2+}$ in which the phenyl groups of the dppe ligand in $\mathbf{1}^{n+}$ are replaced by hydrogen atoms (dpe phosphine). The $\mathbf{1}'^{n+}$ molecular structures are very similar. They have C_i symmetry and are very close to the C_{2h} symmetry which cannot be rigorously satisfied because of the slight twisting of the diphosphine ligand which is necessary to release the metallacycle ring constraint. The optimized molecular structure of $\mathbf{1}'^{2+}$ is shown in Fig. 2. Its frontier MO diagram is shown in Fig. 3. The major geometrical parameters obtained for the $\mathbf{1}^{n+}$ ($n = 0$, 1, 2) series are given in Table 1 together with other computed data. Computed magnetic coupling constants and other relevant data for $\mathbf{1}'^{2+}$ are given in Table 2.

The effect of electron deficiency in $\mathbf{1}'^{2+}$ can be investigated by comparing its structure and charge distribution to those of its reduced states $\mathbf{1}'$ and $\mathbf{1}'^{+}$. In $\mathbf{1}'$, both Fe^{II} centers reach the 18-electron count. The six highest occupied MOs have a large metallic contribution and exhibit some Fe–C and Fe–P π-type bonding character and some Fe–S π-type antibonding character. This is why when going from $\mathbf{1}'$ to $\mathbf{1}'^{+}$ and $\mathbf{1}'^{2+}$ the Fe–C and Fe–P distances increase, whereas the Fe–S distance shortens, the latter variation (≈ 0.14 Å) being significantly larger (see Table 2). This shortening is associated with an increase of the Fe–S–C bond angle. The HOMO of $\mathbf{1}'$, which is the SOMO of $\mathbf{1}'^{+}$, has a 28, 67 and 0% contribution on the $(Fe)_2$, $(S)_2$ and $(CH_2)_2$ units, respectively. The HOMO-1 of $\mathbf{1}'$, which is the SOMO-1 in the triplet state of $\mathbf{1}'^{2+}$, has a 37, 56 and 0% contribution on the $(Fe)_2$, $(S)_2$ and $(CH_2)_2$ units, respectively. These two orbitals are sketched in Scheme 1, projected in the plane containing the Fe and S atoms. They can be described as being the in-phase and out-of-phase combinations of the same 'monomeric' frontier orbitals. Since there is very little interaction between the sulfur π-type orbitals through the saturated organic bridge, there is no reason for the HOMO and HOMO-1 of $\mathbf{1}'$ to be very different in energy. As a matter of fact their energy difference is found to be only 0.17 eV.

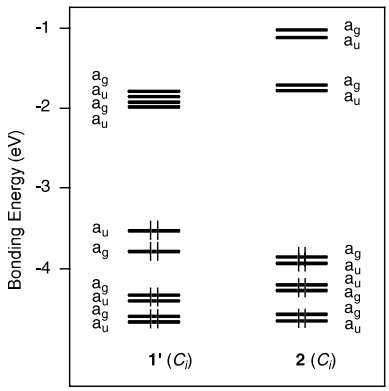

Fig. 3. Frontier MO diagram of $\mathbf{1}'$ and $\mathbf{2}$.

Table 1
Computed major geometrical parameters and energies obtained for $\mathbf{1}'^{0/1+/2+}$ and $\mathbf{2}^{0/1+/2+}$ series

	Fe–X [a]	X–C [a]	C–C	Fe–P	Fe–C(Cp)	Fe–C(Cp) average	Fe–S–C	Fe–S–C–C	ΔE [b] (eV)	E [c] (eV)
$\mathbf{1}'$	2.349	1.881	1.524	2.180–2.180	2.121–2.145	2.134	102.0	171.3	1.557	−286.292
$\mathbf{1}'^{+}$	2.269	1.869	1.523	2.210–2.225	2.149–2.158	2.153	105.0	176.0		−281.828
$\mathbf{1}'^{2+}$ S	2.206	1.867	1.527	2.265–2.247	2.145–2.188	2.168	112.2	175.4	0.160	−278.129
$\mathbf{1}'^{2+}$ S(BS)	2.212	1.881	1.528	2.273–2.247	2.146–2.200	2.174	110.7	179.2	0.952	−278.458
$\mathbf{1}'^{2+}$ T	2.213	1.883	1.528	2.273–2.247	2.145–2.201	2.174	110.3	174.4		−278.429
$\mathbf{2}$	2.098	1.534	1.550	2.160–2.161	2.134–2.148	2.140	114.0	175.0	2.112	−309.150
$\mathbf{2}^{+}$	2.069	1.534	1.551	2.200–2.205	2.136–2.192	2.165	111.9	173.8		−304.451
$\mathbf{2}^{2+}$ S	2.073	1.512	1.652	2.250–2.230	2.147–2.196	2.171	98.0	169.8	0.474	−296.362
$\mathbf{2}^{2+}$ S(BS)	2.054	1.533	1.564	2.261–2.234	2.145–2.228	2.185	104.1	168.7	0.994	−296.707
$\mathbf{2}^{2+}$ T	2.054	1.534	1.555	2.262–2.255	2.141–2.254	2.195	111.4	174.3		−296.718

Distances and angles are given in Å and degrees, respectively. S, Singlet state; BS, broken symmetry; T, triplet state.
[a] X = S in $\mathbf{1}'^{0/1+/2+}$, X = C in $\mathbf{2}^{0/1+/2+}$.
[b] HOMO–LUMO energy gap.
[c] Total bonding energy.

Table 2
Computed spin populations on the iron (P_{Fe}) and sulfur atoms (P_S) in the triplet and broken symmetry states (T and BS, respectively)

	P_{Fe} (T)	P_S (T)	P_{Fe} (BS)	P_S (BS)	S	J_{DFT}	J_S
$\mathbf{1}'^{2+}$	0.704	0.356	0.697	0.334	0.187	−468	−452
$\mathbf{2}^{2+}$	1.120		1.011		0.482	+177	+143

Overlap integral (S) between the two magnetic orbitals evaluated from the spin population on the iron and sulfur centers in the case of $\mathbf{1}'^{2+}$ and the iron centers in the case of $\mathbf{2}^{2+}$ (see text); magnetic coupling constants J_{DFT} and J_S (cm^{-1}).

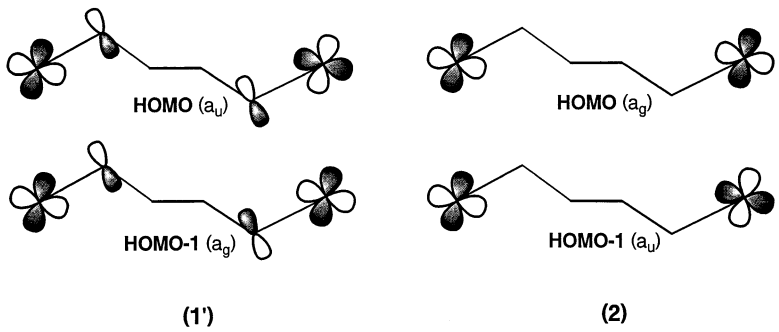

Scheme 1.

The triplet state of $\mathbf{1}'^{2+}$ is computed to be more stable than the delocalized symmetric singlet state. Calculations on the singlet state using the BS technique which allows each spin to preferentially localize on one particular half of the molecule, lead to a stabilization of the singlet state which becomes slightly more stable than the triplet state. This agrees with the antiferromagnetic behavior of $[\mathbf{1}][PF_6]_2$. The computation of accurate magnetic coupling constants J_S of transition–metal complexes is not straightforward. The evaluation of coupling constants of binuclear compounds through DFT calculations has been largely discussed in the litterature [23]. Following the pioneering work of Noodleman on the BS approach [18], new developpements have been recently published [24], which take into account the overlap integral S between the two magnetic orbitals of the BS solution, as given below:

$$J_S = J_{DFT}/(1 + S^2), \text{ where } J_{DFT} = 2(E_{BS} - E_T).$$

An approximate way to evaluate S has been proposed by Blanchet-Boiteux and Mouesca [24b] from the spin population on the metallic centers in the triplet (P_T) and the broken symmetry (P_{BS}) solutions, assuming that the magnetic orbitals have a unique preponderant localization on the metals:

$$S^2 = P_T^2 - P_{BS}^2$$

This simple approximation does not hold for $\mathbf{1}'^{2+}$ for which the magnetic orbitals have significant localization on both the Fe and S centers [24b,24c]. Indeed, each of

the BS magnetic orbitals has 45% localization on one of the S atom and only 33% on the neigboring Fe center. Since there is no simple way provided by the ADF package for the calculation of S, we have used a much rougher approximation, which neglects all the overlap integrals between atomic orbitals, by adding the squares of the Fe and S spin populations, i.e.:

$$S^2 = [P_T(Fe)^2 + P_T(S)^2] - [P_{BS}(Fe)^2 + P_{BS}(Fe)^2]$$

The spin populations have been calculated assuming the Mulliken approximation. They are reported in Table 2 as well as the S, J_{DFT} and J_S values. The computed coupling constant (-452 cm^{-1}) is significantly larger in absolute value than the experimental one (-6.4 cm^{-1}). This difference may arise in part from the modelization of the complex and the method of calculation, but also from the fact that the computed cationic model is considered isolated, while the experimental coupling constant has been determined for the the PF_6^- salt of $\mathbf{1}^{2+}$ in the solid state.

In order to evaluate the role played by the sulfur atoms in the magnetic behavior of $\mathbf{1'}^{2+}$, we have replaced these heteroatoms by saturated CH_2 groups and have calculated the isoelectronic complex ([CpFe(dpe)]$_2$[μ-CH_2–CH_2–CH_2–CH_2–C,C′])$^{2+}$ ($\mathbf{2}^{2+}$), as well as its reduced states $\mathbf{2}^{+}$ and $\mathbf{2}$. The major results are given in Fig. 3, Tables 1 and 2. As expected from the weak π-donor ability of the saturated $(CH_2)_4$ bridge, the HOMO and HOMO-1 of $\mathbf{2}$ have no significant localization on it. They are sketched in Scheme 1, projected in the same plane as those of $\mathbf{1'}$. They both have a 77% contribution on the Fe centers. As a consequence, the oxidation of $\mathbf{2}$ has little effect on the structure of the organic bridge. One should note however that the delocalized symmetric singlet state of $\mathbf{2}^{2+}$ exhibits a particularly long C_β–C_β distance (1.652 Å) asssociated with a particularly small Fe–C_α–C_β angle (98.0°). Thus, this singlet state geometry differs significantly from the one obtained by the BS approach on the same $\mathbf{2}^{2+}$ cation. This is in agreement with the important spin localization on the metal centers found for the BS singlet state of $\mathbf{2}^{2+}$ (Table 2). The energy difference between the triplet and singlet BS states is smaller in $\mathbf{2}^{2+}$ than in $\mathbf{1'}^{2+}$. The calculations predict a ferromagnetic coupling. Clearly, a saturated purely organic bridge linking the metal centers favors a positive coupling constant, while the presence of π-donor heteroatoms at both ends of the bridge tends to favor the opposite situation. Thus, the presence of the donor sulfur atoms in the bridge of complex $\mathbf{1}^{2+}$ is likely to be responsible for the (weak) antiferromagnetism observed in this compound. Finally, it is interesting to note that, contrarily to the $\mathbf{1'}^{+}$ monocation, the isoelectronic binuclear complex ([CpFe(dppe)]$_2$[μ-S–C_5H_4N–N,S])$^{2+}$ exhibits a visible intervalence transition evidencing a considerable electron transfer interaction, but a null magnetic coupling [25]. Preliminary DFT calculations agree with a simple localized picture of a 17-electron Fe center bonded to S and a saturated 18-electron metal bonded to N.

Acknowledgements

Computing facilities were provided by the Centre de Ressourses Informatiques (CRI) of Rennes and the Institut de Développement et de Ressources en Informatique Scientifique du Centre National de la Recherche Scientifique (IDRIS-CNRS). The authors thank the CNRS-CONICYT project PICS 922, FONDAP project 11980002 and FONDECYT project 1000672 for financial support.

References

[1] A.X. Trautwein, Bioinorganic Chemistry: Transition Metals in Biology and Their Coordination Chemistry, Wiley-VCH, Weinheim, 1997.
[2] P.G. Blower, J.R. Dilworth, Coord. Chem. Rev. 76 (1987) 121.
[3] I.G. Dance, Polyhedron 5 (1986) 1037.
[4] J. Lee, G.B. Yi, M.A. Khan, G.B. Richter-Addo, Inorg. Chem. 38 (1999) 4578, and references therein.
[5] G. Lente, X. Shan, I. Guzei, J.H. Espenson, Inorg. Chem. 39 (2000) 3572.
[6] T.D. Stack, M.J. Carney, R.H. Holm, J. Am. Chem. Soc. 111 (1989) 1670.
[7] G.A. Carriedo, A. Arancibia, C. Diaz, N. Yutronic, E.P. Carreño, S.G. Granda, J. Organomet. Chem. 508 (1996) 23.
[8] C. Diaz, A. Arancibia, Inorg. Chim. Acta 269 (1998) 246.
[9] C. Diaz, A. Arancibia, Polyhedron 19 (2000) 137.
[10] C. Diaz, A. Arancibia, Polyhedron 19 (2000) 2679.
[11] C. Diaz, Polyhedron 16 (1997) 999.
[12] (a) E.J. Baerends, D.E. Ellis, P. Ros, Chem. Phys. 2 (1973) 41;
(b) E.J. Baerends, P. Ros, Int. J. Quantum Chem. S12 (1978) 169;
(c) P.M. Boerrigter, G. Velde, E.J. Baerends, J. Int. J. Quantum Chem. 33 (1988) 87;
(d) G. Velde, E.J. Baerends, J. Comput. Phys. 99 (1992) 84.
[13] Vrije Universiteit, Amsterdam, The Netherlands, Amsterdam Density Functional (ADF) program, version 2.3, (1996).
[14] S.D. Vosko, L. Wilk, M. Nusair, Can. J. Chem. 58 (1990) 1200.
[15] H. Stoll, C.M.E. Pavlidou, H. Preuss, Theor. Chim. Acta 49 (1978) 143.
[16] J. Perdew, J.A. Chevary, S.H. Vosko, K.A. Jackson, M.R. Pederson, D.J. Singh, C. Fiolhais, Phys. Rev. Sect., B 46 (1992) 6671.
[17] L. Verluis, T. Ziegler, J. Chem. Phys. 88 (1988) 322.
[18] (a) L. Noodleman, J.G.J. Norman, J. Chem. Phys. 70 (1979) 4903;
(b) L. Noodleman, J. Chem. Phys. 74 (1981) 5737;
(c) L. Noodleman, D.A. Case, Adv. Inorg. Chem. 38 (1992) 423.
[19] A. Earnshaw, Introduction to Magnetochemistry, Academic Press, London and New York, 1968.
[20] C. Diaz, Bol. Soc. Chil. Quim. 44 (1999) 315.
[21] (a) P. Hamon, L. Toupet, J.R. Hamon, C. Lapinte, Organometallics 15 (1996) 10;
(b) T. Weyland, K. Costuas, A. Mari, J.F. Halet, C. Lapinte, Organometallics 17 (1998) 5569;

(c) V. Guillaume, V. Mathias, A. Mari, C. Lapinte, Organometallics 19 (2000) 1422.

[22] F.A. Cotton, G. Wilkinson, Advanced Inorganic Chemistry, 4th ed., Wiley-Interscience, John Wiley & Sons, New York, Chichester, Brisbane, Toronto and Singapore, 1980.

[23] See for example: (a) D. Bencini, D. Gatteschi, F. Totti, D.N. Sanz, J.A. McClaverty, M.D. Ward, J. Phys. Chem. Sect., A 102 (1998) 10545; A. Bencini, I. Ciofini, C.A. Daul, A. Ferretti, J. Am. Chem. Soc. 121 (1999) 11418;
(b) J.E. McGrady, R. Stranger, Inorg. Chem., 38 (1999) 550; C.D. Delfs, R. Stranger, Inorg. Chem. 39 (2000) 491;
(c) E. Ruiz, J. Cano, S. Alvarez, P. Alemany, J. Am. Chem. Soc. 120 (1998) 11122; E. Ruiz, S. Alvarez, P. Alemany, Chem. Comm. (1998) 2767.

[24] (a) R. Caballol, O. Castell, F. Illas, I. De, P.R. Moreira, J.P. Malrieu, J. Phys. Chem., Sect. A 101 (1997) 7860;
(b) C. Blanchet-Boiteux, J.M. Mouesca, J. Phys. Chem., Sect. A 104 (2000) 2091;
(c) E. Ruiz, J. Cano, S. Alvarez, P. Alemany, J. Comput. Chem. 20 (1999) 1391;
(d) C. Blanchet-Boiteux, J.M. Mouesca, J. Am. Chem. Soc. 122 (2000) 861.

[25] C. Diaz, E. Spodine, Y. Moreno, A. Arancibia, Bol. Soc. Chil. Quim. 45 (2000) 317.